PROCEEDINGS OF SPIE

SPIEDigitalLibrary.org/conference-proceedings-of-spie

A carbon nanotube structure for an EUV window with differential pumping

Olson, Scott, Vanfleet, Richard, Allred, David, Turley, Steve, Davis, Robert

Scott Olson, Richard Vanfleet, David Allred, Steve Turley, Robert Davis, "A carbon nanotube structure for an EUV window with differential pumping," Proc. SPIE 11491, Advances in X-Ray/EUV Optics and Components XV, 1149104 (21 August 2020); doi: 10.1117/12.2569049

SPIE.

Event: SPIE Optical Engineering + Applications, 2020, Online Only

Downloaded From: https://www.spiedigitallibrary.org/conference-proceedings-of-spie on 25 Aug 2020 Terms of Use: https://www.spiedigitallibrary.org/terms-of-use

A Carbon Nanotube Structure for an EUV window with Differential Pumping

Scott Olsen, Richard Vanfleet, David Allred, Steve Turley, and Robert Davis

Brigham Young University, Provo, Utah, USA

ABSTRACT

We report on a large-area, high-aspect-ratio, carbon nanotube (CNT) forest structure produced at BYU acting as a window/separator for a hollow cathode EUV lamp. The structure has large-surface-area, high light transmission, and differential pumping. CNT fabrication allows for variable dimensions, which allows various EUV distributions and pressure gradients to be possible. Theory is presented for predicting such distributions and gradients. Several structures have been fabricated; their dimensions, properties, and predicted distributions and gradients are given.

Keywords: Carbon nanotubes, extreme ultraviolet window, differential pumping, EUV lamps

1. INTRODUCTION

All materials absorb extreme ultraviolet (EUV) strongly. This causes difficulty in designing EUV lamps for characterizing equipment for astronomical observations and other applications. Though multilayered mirrors have received much attention for their potential, their fabrication greatly depends on wavelength.[1] Therefore multilayered mirrors cannot be used for a wide bandpass EUV lamp.

2. CARBON NANOTUBE WINDOW

We present a carbon nanotube templated microfabrication (CNT-M) window design for a EUV lamp window that allows high EUV transmission with a wide bandpass. The CNT-M window is infiltrated with carbon for robustness. The versatility of CNT fabrication allows a wide range of distributions. The design restricts gas flow, which allows a pressure difference between the chambers adjacent to the window. We present derivations for the formulae for these properties as functions of CNT-M window dimensions.

2.1 CNT-M Properties

CNT-M devices can have a wide range of properties and applications. Depending on the filler material used in the infiltration step, the device may have high stiffness and high temperature stability. Some of these properties have already been utilized in fabrication electrically actuated switches and doubly clamped beams. While other microfabrication methods, such as DRIE, are limited by compatible materials, CNT-M devices can be infiltrated with many materials, such as metals, polymers, and ceramics.[2]

2.2 Fabrication

CNT-M fabrication was conducted using a process similar to that given by Ref 2.

- HDMS was used as an adhesive for AZ3330 photoresist onto a Al_2O_3 wafer.
- Deposition of a 4 nm iron layer by thermal evaporation onto wafer.
- Liftoff of photoresist using Microposit 1165

For further information:
R.V.: E-mail: rrv3@byu.edu, Telephone: 801 422 1702

Advances in X-Ray/EUV Optics and Components XV, edited by Ali M. Khounsary, Shunji Goto, Christian Morawe, Hidekazu Mimura, Daniele Spiga, Proc. of SPIE Vol. 11491, 1149104
© 2020 SPIE · CCC code: 0277-786X/20/$21 · doi: 10.1117/12.2569049

Downloaded From: https://www.spiedigitallibrary.org/conference-proceedings-of-spie on 25 Aug 2020
Terms of Use: https://www.spiedigitallibrary.org/terms-of-use

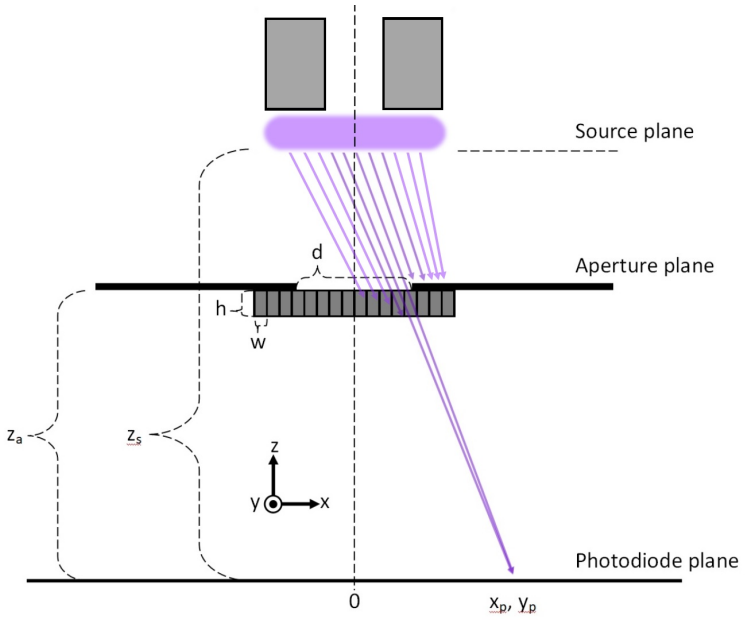


Figure 1: Model for EUV experiment. The intensity observed by a photodiode at x_p, y_p depends on the portion of the cathode (an array of x_s, y_s values) that makes it through the aperture and the CNT-M window.

- CNT growth in quartz tube furnace using atmospheric LPCVD with ethylene at 750 degrees Celsius, followed by carbon infiltration at 900 degrees Celsius for 5 min.
- Plasma etching with an oxygen plasma at 200 W and 40.53 kPa for 5 min for top and bottom of window.
- Release from substrate using KOH solution.

The resulting disk structure is about 3 cm^2, height from about 50 to 1000 microns (determined by duration of CNT growth), wall thickness of 4 microns and pore size of 25, 50, 100, or 200 microns.

3. EXPERIMENTATION

3.1 Theory

3.1.1 EUV Transmission

Figure 1 shows the model. The experiment involves a hollow cathode plasma as an EUV source, which is considered a distributed, uncollimated array of point sources. The intensity at a given position on the viewing plane (x_p, y_p) is then the sum of all the rays from the point sources (x_s, y_s, z_s) that make it through the aperture and the CNT-M window mounted to the aperture, divided by the point source's distance from the position squared:

$$I_{x_p,y_p} = \sum_{s}^{n} \frac{C_s}{(x_s - x_p)^2 + (y_s - y_p)^2 + z_s^2}, \tag{1}$$

where C_s is an intensity function of x_s and y_s, assuming the distribution is nonuniform. The aperture and CNT-M window can be treated as step functions: zero representing where rays are blocked, one representing where rays reach x_p, y_p. Multiplying the cathode distribution by the aperture and CNT-M window step functions then leave the point sources that contribute to I_{x_p,y_p}.

Pillow[3] noted that for a hollow cathode arrangement, given proper conditions the distribution at the cathode is nonuniform. The distribution is a function of pressure, current, and wavelength being observed. The cathode

Downloaded From: https://www.spiedigitallibrary.org/conference-proceedings-of-spie on 25 Aug 2020
Terms of Use: https://www.spiedigitallibrary.org/terms-of-use

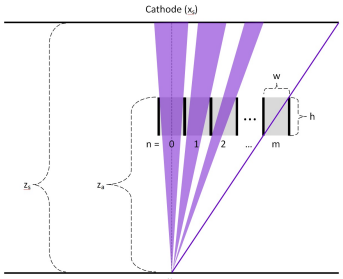


Figure 2: "Center" position of CNT-M window.

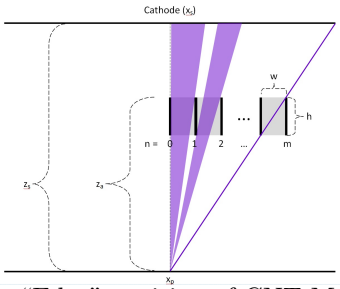


Figure 3: "Edge" position of CNT-M window.

is modelled as a planar source at the end of the cathode using a quartic equation with the constraints of $I = 0$ at radius R from the center axis of the cathode, and $I_{max} = 1$. Doing so yields

$$I(r) = \frac{-4R^2(R^2r^2 + c)(r^2 - R^2)}{(R^4 + c)^2} \tag{2}$$

for a distance r from the cathode axis, with $0 \leq c \leq R^4$. The constant c reflects the change in pressure, current, and wavelength being observed, which determines the "shape" of the distribution. Given the current and wavelength are fixed, we expect c to decrease in value with increasing pressure. c as a function of pressure is to be determined by observing distributions. With c, the distribution at the cathode is then written into an 1,201 x 1,201 array, which corresponds to a 30mm x 30mm area with 25 micron steps.

To determine the step function for the aperture, we consider a ray from x_s, y_s, passing through the plane of the aperture (x_a, y_a), and arriving at x_p, y_p. Then finding x_s, y_s as a function of x_a, y_a and x_p, y_p, and constricting the location of ones on x_s, y_s by constricting x_a, y_a to within an aperture yields:

$$x_s = x_p + \frac{z_s}{z_a}(x_a - x_p) \tag{3}$$

$$y_s = y_p + \frac{z_s}{z_a}(y_a - y_p) \tag{4}$$

where $\frac{-d}{2} \leq x_a \leq \frac{d}{2}$ and $-\sqrt{\frac{d^2}{4} - x_a^2} \leq y_a \leq \sqrt{\frac{d^2}{4} - x_a^2}$ for a circular aperture of diamater d, assuming the center axis of the aperture is aligned with the center axis of the hollow cathode. The step function is then written as a 1,201 x 1,201 array as a function of x_p, y_p.

The step function for the CNT-M window considers two effects, shown in both Figures 2 and 3: the inner walls blocking rays (which creates bands of contributing point sources on the cathode), and the collimating angle (beyond which no point sources contribute).

The inner wall blocking is dependent on the position of the window with respect to x_p, y_p. We consider two positions: x_p, y_p is underneath the center of a column (Fig 2), and x_p, y_p is underneath a wall or "edge" (Fig 3). In both positions, the walls of the window are assumed to be parallel to the x and y axis on the viewing plane. For "center" position, the x_s values with rays directed to x_p that strike the top and bottom of the window walls are, respectively:

$$x_s = x_p + \frac{z_s w}{z_a}(n + 1/2) \tag{5}$$

$$x_s = x_p + \frac{z_s w}{z_a - h}(n - 1/2) \tag{6}$$

where n is the nth column from the column directly above x_p. To the right of x_p, the x_s are given by Eq 6$\leq x_s \leq$ Eq 5. If the sign following x_p is reversed in both equations, then for pores to the left of x_p Eq 5$\leq x_s \leq$Eq 6. For the column directly above x_p, we have Eq 5$(n = -1) \leq x_s \leq$Eq 5$(n = 0)$. Values for y_s follow the same procedure. For "edge" position, n represents the nth wall from the wall directly above x_p. Eq 5 and Eq 6 then become, respectively:

$$x_s = x_p + \frac{z_s w}{z_a}(n + 1) \tag{7}$$

Downloaded From: https://www.spiedigitallibrary.org/conference-proceedings-of-spie on 25 Aug 2020
Terms of Use: https://www.spiedigitallibrary.org/terms-of-use

$$x_s = x_p + \frac{z_s w n}{z_a - h} \tag{8}$$

To the right Eq 8$\leq x_s \leq$Eq 7. Reversing the signs again, to the left Eq 7 $\leq x_s \leq$ Eq 8. We consider the wall directly above x_p to be infinitely thin, therefore directly above x_p Eq 7$(n = -2) \leq x_s \leq$ Eq 7$(n = 0)$.

The collimating angle occurs at the mth column- where a ray would strike the top of a wall and the bottom of the previous wall. Substituting m for n into the appropriate equations for top and bottom, setting the two equal to each other, and solving for m, yields:

$$m = \frac{z_a}{h} - \frac{1}{2} \tag{9}$$

for the "center" position, and

$$m = \frac{z_a}{h} - 1 \tag{10}$$

for "edge" position. In general, we define "x-center, y-edge" as a "center" position along the x axis and an "edge" position along the y axis above the point $x_p, y_p = 0, 0$; "x-edge, y-center", "both-center", and "both-edge" in like manner.

Given the position, column width and height, and x_p, y_p, a 1,201 x 1,201 array is written representing the window.

The cathode array, aperture array, and CNT-M window array are multiplied element-wise. The remaining nonzero elements represented the point sources on the cathode that make it through the aperture and window to x_p, y_p. Each element is substituted into Eq.1 for C_s. Done over an array of x_p, y_p values and normalized to the maximum intensity value yields the expected EUV distribution.

3.1.2 Pressure Ratio

We derive the expected pressure ratio of the two sides of the CNT-M window by first calculating its conductance, then measuring the conductance of the restrictor the CNT-M window is mounted to, adding these conductances in series and dividing by the pumping speed. We assume molecular flow regime so that the conductance is purely a geometric property.

We first consider the conductance of a single pore. The conductances of the opening and length of the pore in L/s are given by 4 with T for temperature in Kelvin, M for the molecular weight of the gas in kg/mol, h and w the height and width of the column in cm, respectively:

$$C_{opening} = 3.64 w^2 \sqrt{\frac{T}{M}} \tag{11}$$

$$C_{length} = 9.70 \frac{w^3}{2h} \sqrt{\frac{T}{M}} \tag{12}$$

The conductance of one pore is then:

$$C_{pore} = \frac{1}{\frac{1}{C_{opening}} + \frac{1}{C_{length}}} \tag{13}$$

$$C_{total} = \frac{1}{\frac{1}{C_{window}} + \frac{1}{C_{aperture}}} \tag{14}$$

We add in parallel the number of pores, which is approximated as the area of the aperture ($A_{aperture}$) the CNT-M window is mounted to divided by the open area of one pore:

$$C_{window} = N_{pores} C_{pore} \approx \frac{A_{aperture}}{A_{pore}} C_{pore} = \frac{A_{aperture} C_{pore}}{(w+t)^2} \approx \frac{A_{aperture}}{0.275 + 0.206 \frac{h}{w}} \sqrt{\frac{T}{M}} \tag{15}$$

Downloaded From: https://www.spiedigitallibrary.org/conference-proceedings-of-spie on 25 Aug 2020
Terms of Use: https://www.spiedigitallibrary.org/terms-of-use

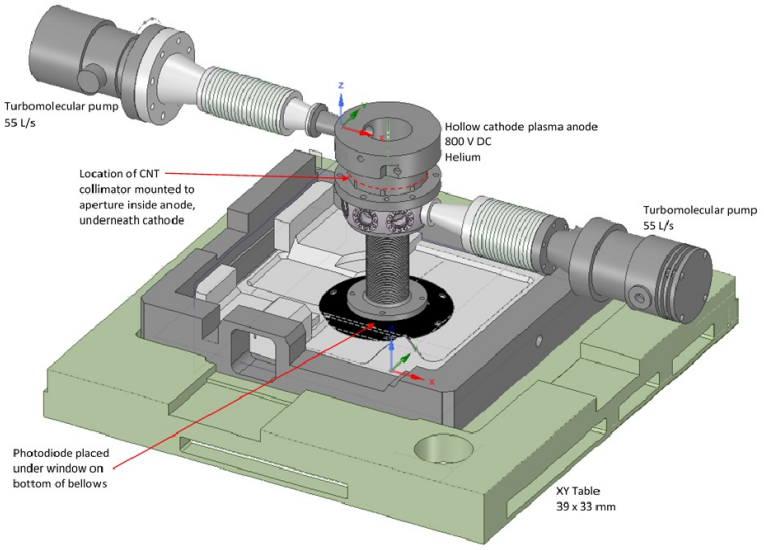


Figure 4: Diagram of EUV experiment. Pressure gauges, stepper motors for xy table, and photodiode are not shown.

Assuming the wall thickness t is much less than w. We then add the measured conductance of the aperture:

$$C_{total} = \frac{1}{\frac{1}{C_{window}} + \frac{1}{C_{aperture}}} = \frac{A_{aperture}}{(0.275 + 0.206\frac{h}{w})\sqrt{\frac{M}{T}} + \frac{A_{aperture}}{C_{aperture}}} \tag{16}$$

The pressure ratio across is given by:

$$\frac{P_L}{P_H - P_L} \approx \frac{P_L}{P_H} = \frac{C_{total}}{S} \tag{17}$$

Where S is the pumping speed in L/s, and P_L and P_H are the low and high pressures in torr, respectively,[4] and assuming $P_L << P_H$. The result is:

$$\frac{P_L}{P_H} \approx \frac{1}{S} \times \frac{A_{aperture}}{(0.275 + 0.206\frac{h}{w})\sqrt{\frac{M}{T}} + \frac{A_{aperture}}{C_{aperture}}} \tag{18}$$

3.2 Setup

Figure 4 shows the setup for testing EUV transmission and pressure ratio. A hollow cathode helium DC plasma, run at 800 V at 1 torr and below, acts as an EUV source (58.4 nm). The anode is connected to a micropirani gauge (not shown in Figure 4, 1e-5 to 760 torr) and a turbomolecular pump (55 L/s). 38.3 mm below the cathode, at the base of the anode the CNT-M window is mounted to an aperture. Below the anode a chamber with a bellows is connected to a second micropirani gauge and turbomolecular pump. The base of the bellows has a window mounted to an xy table (30mm x 30 mm range), under which is a photodiode. The photodiode will scan across the visible light distribution. The window will then be coated with a phosphur to observe the EUV distribution. The gauges allow the pressure ratio to be observed.

Given the dimensions of the xy table limit scanning angle, and a desired maximum pressure ratio of $P_L/P_H = 0.1/1$ torr $= 0.1$, aperture conductance is ignorable ($C_{aperture} = \infty$), we calculated possible CNT-M window dimensions, given in Table 1. CNTs become difficult to grow past 1000 microns, therefore we limit to 50 micron and 25 micron windows. Note that these dimensions are for the maximum pressure ratio; therefore windows of greater heights may also be considered.

The CNT-M window may be close enough to the plasma that etching was a concern. If etching is significant, the height (and therefore the distribution and pressure ratio) would vary during a given trial. Heights and window conditions will then be measured after each trial.

Downloaded From: https://www.spiedigitallibrary.org/conference-proceedings-of-spie on 25 Aug 2020
Terms of Use: https://www.spiedigitallibrary.org/terms-of-use

Table 1: CNT-M window dimensions necessary for maximum pressure ratio within limiting aperture and scanning angle. All values are rounded up to the nearest micron. The range in height and θ_c are to account for uncertainty in temperature of plasma. The ranges are calculated from 300 K to 500 K.

Width (microns)	Height (microns)	θ_c (degrees)	Radius (cm)
25	530↔578	2.70↔2.48	0.172↔0.158
50	1060↔1156	2.70↔2.48	0.172↔0.158
100	2119↔2312	2.70↔2.48	0.172↔0.158
200	4238↔4623	2.70↔2.48	0.172↔0.158

Table 2: CNT-M window dimensions

Window	Pore Size (microns)	Initial Height (microns)
A	25	950 ± 8
B	25	1138 ± 20
C	50	1182 ± 13

3.3 Data and Discussion

Three CNT-M windows were fabricated and mounted to a 3.3 mm diameter, 3.2 mm thick aperture using epoxy. Initial heights were measured are listed in Table 2. The surface within the aperture of the windows was imaged using an SEM (Figures 5 thru 7).

3.3.1 EUV Transmission

With $z_s = 254.3$, $R = 12.5$, $z_a = 216$, $d = 3.3$ mm, and $c = R^4$, we calculated expected EUV distribution of CNT-M windows A, B, and C (Figures 8 thru 10; x and y axes are in mm). Figure 11 shows the four positions ("x-center, y-edge", "x-edge, y-center", "both-center," "both-edge") for window A. We observed that the difference between positions is negligible.

3.3.2 Pressure Ratio

To measure $C_{aperture}$ in Eq 18, an aperture without a CNT-M window mounted was inserted and the pressure ratio observed. Multiplying the ratio by the pumping speed gives the approximate conductance of the aperture. Twenty data points were recorded 30 s apart at each high pressure of about 500, 650, and 800 mtorr of helium. No plasma was present. Figure 12 shows that the conductance is a function of pressure, implying the gas is in the viscous flow regime. A linear fit to the data gives:

$$C_{aperture} = 23.05 \times P_h + 3.39 \tag{19}$$

with P_h in torr and $C_{aperture}$ in torrL/s. Substituting this into Eq 18, the pressure ratios of each window as functions of P_h and temperature were calculated (Figures 13 thru 15).

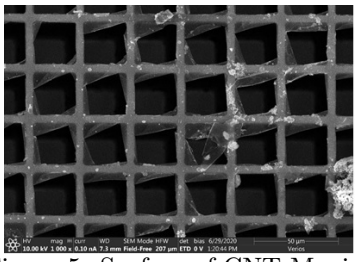


Figure 5: Surface of CNT-M window A within 3.3 mm aperture.

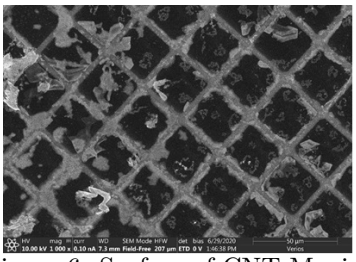


Figure 6: Surface of CNT-M window B within 3.3 mm aperture.

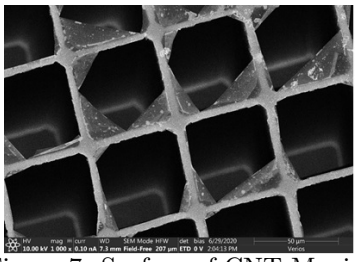


Figure 7: Surface of CNT-M window C within 3.3 mm aperture.

Downloaded From: https://www.spiedigitallibrary.org/conference-proceedings-of-spie on 25 Aug 2020
Terms of Use: https://www.spiedigitallibrary.org/terms-of-use

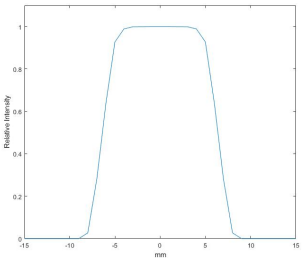


Figure 8: Predicted EUV distribution of CNT-M window A along y axis, "both-center" position.

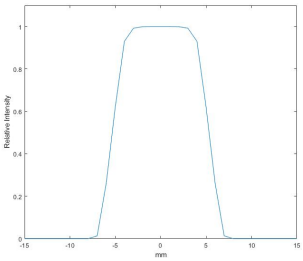


Figure 9: Predicted EUV distribution of CNT-M window B along y axis, "both-center" position.

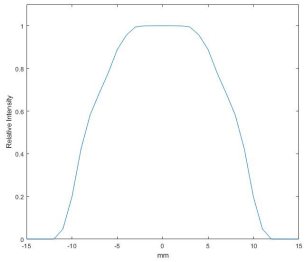


Figure 10: Predicted EUV distribution of CNT-M window C along y axis, "both-center" position.

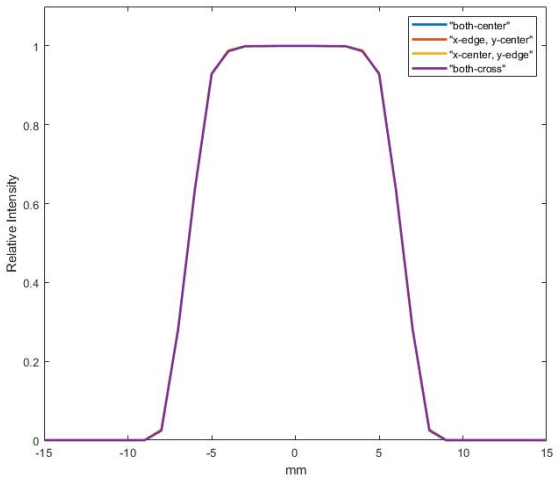


Figure 11: Distributions of window A with "both-center", "x-center, y-edge", "x-edge, y-center", and "both-edge". Note the variation between distributions is negligible.

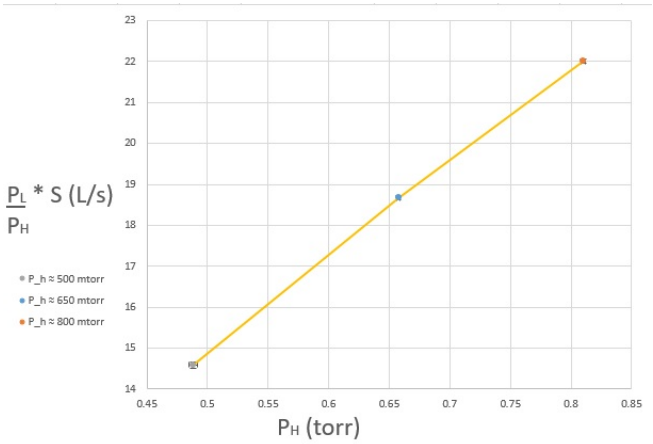


Figure 12: Conductance of 3.3 mm diameter, 3.2 mm thick aperture with helium at various pressures and a 55 L/s turbo pump. Three P_h values, with twenty data points each, were observed. Averages are plotted. Error bars are standard deviation: horizontal $\approx$ 0.003, 0.002, and 0.002; vertical $\approx$ 0.079, 0.052, and 0.047 for $P_h \approx$ 500, 650, and 800 mtorr, respectively

Downloaded From: https://www.spiedigitallibrary.org/conference-proceedings-of-spie on 25 Aug 2020
Terms of Use: https://www.spiedigitallibrary.org/terms-of-use

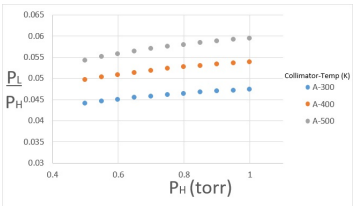


Figure 13: Predicted pressure ratio of CNT-M window A as a function of high pressure and temperature.

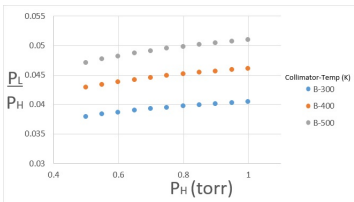


Figure 14: Predicted pressure ratio of CNT-M window B as a function of high pressure and temperature.

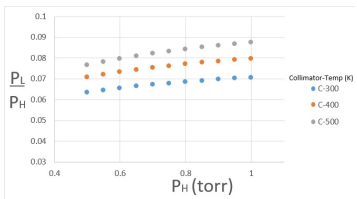


Figure 15: Predicted pressure ratio of CNT-M window C as a function of high pressure and temperature.

4. CONCLUSION

We have developed a CNT-M EUV window that allows EUV transmission, as well as gas restriction. The versatility of CNTs allow the window to have variable dimensions, which then determine the EUV transmission and gas restriction. Coupled with theory, the window can be designed for many applications. We intend to demonstrate the window's applicability as an essential component of an EUV lamp.

ACKNOWLEDGMENTS

We like to thank the BYU Graduate Studies HIDRA Fellowship and the BYU Physics and Astronomy Department for funding, John Ellsworth and the BYU Physics Machine Shop for EUV experiment design and fabrication, BYU IMF for providing necessary equipment and materials for fabrication of windows, and BYU Microscopy for SEM images. This research was also supported in part through the Utah NASA Space Grant Consortium, NASA Grant #NNX15AI24H.

REFERENCES

[1] Bourassin-Bouchet, C., de Rossi, S., and Delmotte, F., [*Optical Technologies for Extreme-Ultraviolet and Soft X-ray Sources*], vol. 197 of *Springer Series in Optical Sciences*, ch. 8, 151–173, McGraw-Hill (2015).

[2] Hutchison, D. N., Morrill, N. B., Aten, Q., Turner, B. W., Jensen, B. D., Howell, L. L., Vanfleet, R. R., and Davis, R. C., "Carbon nanotubes as a framework for high-aspect-ratio mems fabrication," *Journal of Microelectromechanical Systems* **19**(1), 75–82 (2010).

[3] Pillow, M., "A critical review of spectral and related physical properties of the hollow cathode discharge," *Spectrochimica Acta Part B: Atomic Spectroscopy* **36**(8), 821 – 843 (1981).

[4] Ohring, M., [*Materials Science of Thin Films*], Academic Press (2002).

Downloaded From: https://www.spiedigitallibrary.org/conference-proceedings-of-spie on 25 Aug 2020
Terms of Use: https://www.spiedigitallibrary.org/terms-of-use